

Inverted Oscillators for Testing Gravity-induced Quantum Entanglement

Tomohiro Fujita,^{1,2,*} Youka Kaku,^{3,†} Akira Matumura,^{4,‡} and Yuta Michimura^{5,2,§}

¹*Waseda Institute for Advanced Study, Waseda University,
1-6-1 Nishi-Waseda, Shinjuku, Tokyo 169-8050, Japan*

²*Research Center for the Early Universe, The University of Tokyo, Bunkyo, Tokyo 113-0033, Japan*

³*Department of Physics, Graduate School of Science,
Nagoya University, Chikusa, Nagoya 464-8602, Japan*

⁴*Department of Physics, Kyushu University, Fukuoka, 819-0395, Japan*

⁵*LIGO Laboratory, California Institute of Technology, Pasadena, California 91125, USA*

In the quest for quantum gravity, we have lacked experimental verification, hampered by the weakness of gravity and decoherence. Recently, various experiments have been proposed to verify quantum entanglement induced by Newtonian gravitational interactions. However, they are not yet certainly feasible with existing techniques. To search for a new setup, we compute the logarithmic negativity of two oscillators with arbitrary quadratic potential coupled by gravity. We find that unstable inverted oscillators generate gravity-induced entanglement most quickly and are most resistant to decoherence from environmental fluctuations. As an experimental realization, we propose a setup of the optical levitation of mirrors with the anti-spring effect. To avoid decoherence due to photon shot noise, a sandwich configuration that geometrically creates the anti-spring is promising.

I. INTRODUCTION

Quantum gravity has been one of the biggest challenges in modern physics for a long time [1, 2]. The lack of experiments has made its construction more intractable. It is not even confirmed whether a gravitational field can be in a quantum superposition state. Recently, some experimental proposals were made and have attracted much attention [3, 4]. These experiments aim to measure the quantum entanglement produced by the Newtonian gravitational interaction between two masses. Following them, many proposals using matter-wave interferometers [5–10], mechanical oscillator model [11, 12], optomechanical systems [13–19] and their hybrid model [20–24] were studied.

Among these proposals, the authors of Ref. [11] found that entanglement generation occurs simply by trapping two masses in a potential and then releasing them. This is because as their wavefunctions spread out after the release, the near side feels relatively strong gravity and the far side feels weak gravity, resulting in non-local quantum correlations. However, two problems were pointed out in a follow-up paper [25]: one, as with other proposals, requires strong suppression of environmental noise such as air molecule scattering to avoid decoherence until measurable entanglement is produced. The other is that unless the experiment is conducted in space with microgravity, the masses will free-fall after potential release. For three seconds, they will fall more than 40 meters down, making the measurement of the generated entanglement difficult. This free-fall problem is a serious issue because if mechanical support is introduced to prevent the masses from falling, large thermal noise through the support would lead to rapid decoherence.

Furthermore, in common with classical experiments, the weakness of gravity is an obstacle. The dimensionless

parameter of gravity acting on two identical oscillators with mass m and angular frequency ω placed at distance d is

$$\eta \equiv \frac{2Gm}{\omega^2 d^3} = 2.7 \times 10^{-13} \omega_{\text{kHz}}^{-2} \left(\frac{m/d^3}{2 \text{ g/cm}^3} \right), \quad (1)$$

where we introduced $\omega_{\text{kHz}} \equiv \omega/1\text{kHz}$ and m/d^3 is roughly capped by the density of the oscillators. Since we will consider an optomechanical setup, we have chosen 2g/cm^3 as our fiducial value, referring to the typical density of the mirror material such as fused silica (2.2 g/cm^3) or silicon (2.3 g/cm^3). To obtain a measurable signal, we have to overcome the smallness of η .

In this paper, we seek a new experimental setup addressing the above problems. We first provide a generic theoretical framework to consider the gravitational interaction between oscillators. We consider a pair of oscillators with arbitrary quadratic potentials and investigate when the generated entanglement is maximized. By computing logarithmic negativity, we find that unstable inverted oscillators generate entanglement most quickly. Their entanglement increases exponentially, which is advantageous for overcoming weak gravity. They can also potentially relax decoherence requirements because only a short time is needed to generate measurable entanglement. We then explore the experimental realization of such inverted oscillators. The milligram mass range is known to be promising for experimental verification of the quantum nature of gravity [26–28]. In that region, the anti-spring effects in cavity optomechanics are well known and practiced [29, 30]. To avoid decoherence due to photon shot noise, we will consider a sandwich configuration of mirrors [31].

II. OSCILLATORS WITH ARBITRARY QUADRATIC POTENTIAL

In this section, we solve the dynamics of two oscillators with arbitrary quadratic potential and calculate the quantum entanglement between them induced by gravity. We consider a general Hamiltonian for two oscillators coupled by Newtonian gravity,

$$H = \frac{p_1^2}{2m} + \frac{1}{2}k_1x_1^2 + \frac{p_2^2}{2m} + \frac{1}{2}k_2x_2^2 - \frac{Gm^2}{d^3}(x_1 - x_2)^2, \quad (2)$$

where k_i ($i = 1, 2$) is spring constant and we keep only relevant interaction terms by assuming $d \gg |x_i|$. Introducing dimensionless variables, $P_i \equiv p_i/\sqrt{\hbar m\omega}$, $X_i \equiv \sqrt{m\omega/\hbar}x_i$, the above Hamiltonian is rewritten as

$$H = \frac{\omega}{2} \left[P_1^2 + \lambda_1 X_1^2 + P_2^2 + \lambda_2 X_2^2 - \eta (X_1 - X_2)^2 \right], \quad (3)$$

where the new constant parameters $\lambda_i \equiv k_i/(m\omega^2)$ specify the potentials. When λ_i is $+1, 0$, and -1 , the potential becomes harmonic, free and inverted, respectively. Here ω appeared independent of the other parameters, the meaning of which will be described soon below.

The Heisenberg-Langevin equations for the coupled oscillators read

$$\dot{X}_i = \omega P_i, \quad \dot{P}_i = -\lambda_i \omega X_i + \omega \eta (X_i - X_j) + \xi_i, \quad (4)$$

where $i, j = 1$ or 2 , $i \neq j$, and a random force noise ξ_i is added to incorporate environmental fluctuations, while the small dissipation term is ignored [11, 25]. We assume ξ_i is a white noise and its amplitude is characterized by a parameter μ as

$$\frac{1}{2} \langle \xi_i(t) \xi_j(t') + \xi_i(t') \xi_j(t) \rangle = \mu \omega \delta(t - t') \delta_{ij}. \quad (5)$$

The details of μ and the validity of this treatment will be discussed in the next section.

Since we consider the quadratic potentials, Eq. (4) is exactly solvable. The derivation is described in Appendix A. We introduce a vector of the dynamical variables and a covariance matrix,

$$u_i(t) = \left(X_1(t), P_1(t), X_2(t), P_2(t) \right), \quad (6)$$

$$\sigma_{ij}(t) = \frac{1}{2} \langle u_i(t) u_j(t) + u_j(t) u_i(t) \rangle. \quad (7)$$

Here we consider $\langle u(0) \rangle = 0$ and $\sigma_{ij}(0) = \delta_{ij}/2$ as an initial condition. It implies that the two oscillators are in the ground state of the harmonic potential with a common frequency ω at $t = 0$, irrespective of λ_i , and then they evolve with their spring constants $\lambda_i m \omega^2$ for $t > 0$. Without introducing trapping potentials of ω , the initial state for $\lambda_i \leq 0$ would be ill-defined.

Having the solution $\sigma_{ij}(t)$, one can define $\tilde{\sigma}_{ij}(t)$ by flipping the sign of the oscillator's momentum P_2 and compute the so-called minimum symplectic eigenvalue $\tilde{\nu}_{\min}$ from $\tilde{\sigma}_{ij}(t)$. The explicit form is

$$\tilde{\nu}_{\min} \equiv \left[\frac{1}{2} \left(\tilde{\Sigma} - \sqrt{\tilde{\Sigma}^2 - 4 \det \sigma} \right) \right]^{1/2}, \quad (8)$$

where $\tilde{\Sigma} \equiv \det \sigma_1 + \det \sigma_2 - 2 \det \sigma_3$ with the 2×2 matrices σ_1, σ_2 and σ_3 appearing in the block form of $\sigma(t)$,

$$\sigma(t) = \begin{bmatrix} \sigma_1 & \sigma_3 \\ \sigma_3^T & \sigma_2 \end{bmatrix}. \quad (9)$$

It is known that $\tilde{\nu}_{\min} < 1/2$ is a necessary and sufficient condition for the two oscillators to be entangled [32–36]. To quantify the generated entanglement, the logarithmic negativity,

$$E_N \equiv \max[0, -\log_2(2\tilde{\nu}_{\min})], \quad (10)$$

is useful. When $E_N > 0$, the oscillators are entangled, and larger E_N indicates larger entanglement. Entanglement between a mechanical oscillator and microwave has been measured experimentally with an accuracy of $\mathcal{O}(10^{-2})$ [37]. Hence, in this paper, we set our target negativity as $E_N = 10^{-2}$.

In Fig. 1, we present the logarithmic negativity E_N of the two generic oscillators. We observe that a pair of the inverted oscillators generate the largest negativity, while virtually no negativity is produced if either one of the oscillators has positive λ_i . Since no special point is found in the off-diagonal region of the contour plot, we restrict ourselves to the cases with two identical oscillators by setting $\lambda \equiv \lambda_1 = \lambda_2$ (on the diagonal line in Fig. 1) in the rest of this paper.

For two identical oscillators, by expanding the logarithmic negativity with respect to $\eta \sim \mu \ll 1$, we obtain a readable result,

$$E_N(t) \simeq 3 \left[\eta f_{\text{gra}}(t) - \mu f_{\text{dec}}(t) \right], \quad (11)$$

where the right-hand side is assumed to be positive. The gravitational term ηf_{gra} tries to generate the entanglement but the decoherence term μf_{dec} tries to prevent it. The full expressions for f_{gra} and f_{dec} are written in Appendix A (see Eq. (29)). In the short time limit $\omega t \ll 1$, they merge to $f_{\text{gra}} \simeq f_{\text{dec}} \simeq \omega t/2$ irrespective to λ . In the long time limit $\omega t \gg 1$, for $\lambda = \pm 1$ and 0 , we find

$$f_{\text{gra}} \simeq \begin{cases} \frac{1}{2} |\sin(\omega t)| \\ \frac{1}{6} (\omega t)^3 \\ \frac{1}{8} e^{2\omega t} \end{cases}, \quad f_{\text{dec}} \simeq \begin{cases} \frac{1}{2} \omega t & (\lambda = 1) \\ \frac{1}{6} (\omega t)^3 & (\lambda = 0) \\ \frac{1}{8} e^{2\omega t} & (\lambda = -1) \end{cases}. \quad (12)$$

For $\lambda \leq 0$, f_{gra} and f_{dec} have the same asymptotic behavior again, and Eq. (11) is further approximated by

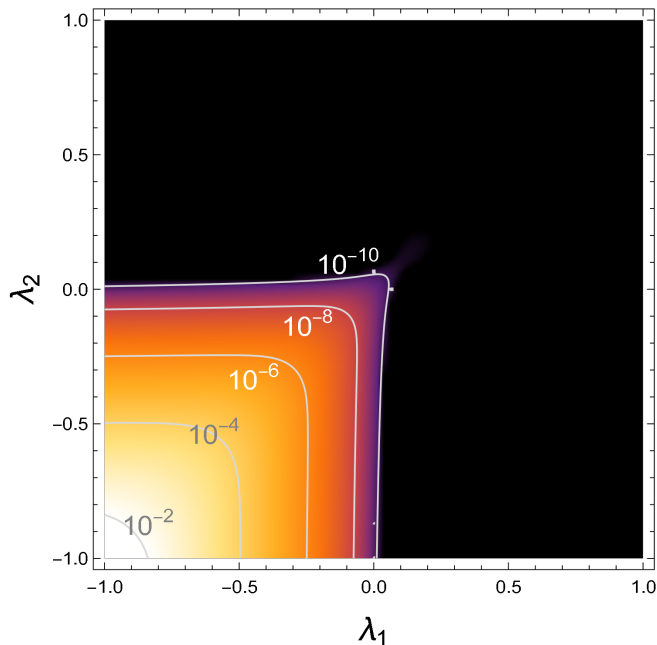


FIG. 1: The logarithmic negativity E_N of the two oscillator systems induced by the gravitational interaction. We choose $\omega t = 13$ and $\eta = 2\mu = 10^{-12}$. The horizontal (λ_1) and vertical (λ_2) axes denote the potential form of the two oscillators (see Eq. (3)) and $\lambda_i = +1, 0, -1$ corresponds to harmonic, free and inverted quadratic potential, respectively. The largest negativity is generated when both oscillators have the inverted potential (the left bottom corner).

$E_N \simeq 3(\eta - \mu)f_{\text{gra}}$. Thus, for entanglement generation, it is necessary to suppress the decoherence effect μ . This fact was known in previous study only for $\lambda = 0$ in the short time limit [25], but we generalize it for $\lambda \leq 0$ in the long time limit.

Fig. 2 shows the time evolution of f_{gra} and f_{dec} for $\lambda = \pm 1$ and 0. The exponential growth of f_{gra} in the case of the inverted oscillator is remarkable. To overcome the weakness of gravity ($\eta \ll 1$) and achieve detectable negativity $E_N = 10^{-2}$, f_{gra} has to quickly increase to a huge value $\simeq 10^{-2}/3\eta$, before the environmental fluctuations decohere the system. Combining Eqs. (1), (11), (12) and neglecting μ for a moment, we obtain the time required to generate the entanglement as

$$\tau_{\text{ent}} \simeq \begin{cases} 4.2 \omega_{\text{kHz}}^{-1/3} \text{ sec} & (\lambda = 0) \\ 1.3 \times 10^{-2} \omega_{\text{kHz}}^{-1} \text{ sec} & (\lambda = -1) \end{cases}. \quad (13)$$

The inverted oscillators are roughly three hundred times faster than the free masses at $\omega = 1\text{kHz}$ and the difference is even greater for larger ω . Moreover, taking into account the decoherence parameter μ , τ_{ent} elongates by a factor of $[\eta/(\eta - \mu)]^{1/3}$ for $\lambda = 0$, while only $\log[\eta/(\eta - \mu)]/(2\omega) = \mathcal{O}(10^{-3})\omega_{\text{kHz}}^{-1}\text{sec}$ is added to Eq. (13) in the $\lambda = -1$ case. Therefore, the inverted oscillators generate the gravity-induced entanglement most

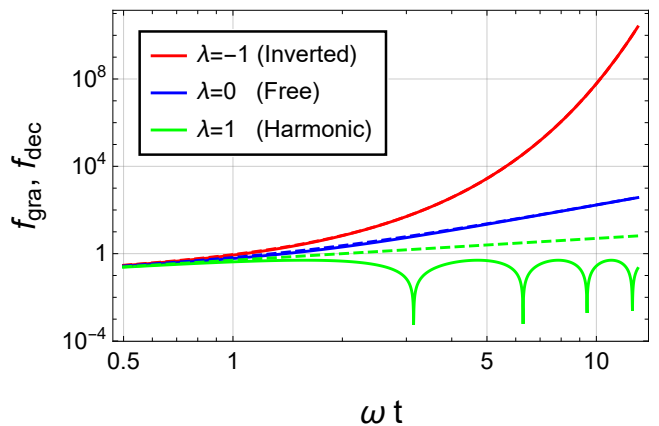


FIG. 2: Time evolution of f_{gra} introduced in Eq. (11) for $\lambda = -1$ (red), 0 (blue), and 1 (green) against ωt . f_{dec} is also shown as dashed line but almost overlapped with f_{gra} except for $\lambda = 1$. f_{gra} converge to $\omega t/2$ in the short time limit irrespective to λ . In the long time regime, however, the increasing rate of f_{gra} is largely dependent on λ . The inverted oscillators are particularly prominent for their exponential growth.

quickly and are most resistant to decoherence.

III. DECOHERENCE AND THE TIME SCALE OF THE ENTANGLEMENT GENERATION

According to the analysis of the previous section, it appeared as if the suppression of decoherence down to $\mu < \eta$ was an unavoidable condition for the entanglement generation because $E_N \simeq 3(\eta - \mu)f_{\text{gra}}$ in the long time regime. However, this is not necessarily the case, if the entanglement generation occurs fast enough.

One of the main sources of the decoherence effect is interaction with air molecules. In terms of the decoherence parameter μ , this process is expressed as [38]

$$\begin{aligned} \mu_{\text{air}} &= \frac{16pR^2}{3\hbar m\omega^2} \sqrt{2\pi m_{\text{air}} k_B T}, \\ &= 4 \times 10^{-13} \omega_{\text{kHz}}^{-2} \left(\frac{p}{10^{-17}\text{Pa}} \right) \left(\frac{T}{1\text{K}} \right)^{\frac{1}{2}} \left(\frac{R}{0.2\text{mm}} \right)^2, \end{aligned} \quad (14)$$

where R is the radius of the oscillator, p and T are the pressure and temperature of the environment, and we used the mass of nitrogen molecule $m_{\text{air}} = 4.7 \times 10^{-23}\text{g}$ and $m = 0.1\text{mg}$. To achieve $\mu_{\text{air}} < \eta$, we need extremely high vacuum, $p \lesssim 10^{-17}\text{Pa}$. Thus, the sufficient suppression of decoherence is a major challenge, as pointed out in a previous study.

Nonetheless, even if μ_{air} is larger than η , decoherence should be ineffective, if no scattering occurs during the experiment. How often do the air molecules actually hit

the oscillator? The mean free time of the scattering between the oscillator and the molecules is evaluated as

$$\begin{aligned}\tau_{\text{air}} &= (\pi R^2 v_x n_{\text{air}})^{-1}, \\ &= 0.64 \text{ sec} \left(\frac{R}{0.2 \text{ mm}} \right)^{-2} \left(\frac{p}{10^{-17} \text{ Pa}} \right)^{-1} \left(\frac{T}{1 \text{ K}} \right)^{\frac{1}{2}},\end{aligned}\quad (15)$$

where $n_{\text{air}} = p/k_B T$ is the molecule density and $v_x = \sqrt{k_B T/m_{\text{air}}}$ is its velocity in one direction. Note that τ_{air} is much longer than τ_{ent} of the inverted oscillators in Eq. (13). Roughly requiring $\tau_{\text{air}} \gtrsim \tau_{\text{ent}}$, we find the maximum allowed value of the pressure for the inverted oscillators as

$$p \lesssim 5.3 \times 10^{-16} \text{ Pa } \omega_{\text{kHz}} \left(\frac{R}{0.1 \text{ mm}} \right)^{-2} \left(\frac{T}{1 \text{ K}} \right)^{\frac{1}{2}}. \quad (16)$$

Extremely low pressure at the level of $p \simeq 10^{-16} \text{ Pa}$ has been experimentally achieved [39]. Although the higher temperature is apparently favorable, other decoherence processes such as thermal photon scattering would be significant. Consequently, the inverted oscillators can potentially relax the ultrahigh vacuum requirement and make the experiment more realistic by increasing ω . For a more rigorous treatment, one should revisit the Heisenberg-Langevin equations (4) and go beyond the Markovian random force approximation of ξ_i .

IV. EXAMPLE OF EXPERIMENTAL REALIZATION

So far, we have examined the coupled oscillators for gravity-induced entanglement on a theoretical basis. In this section, we explore an experimental realization of inverted oscillators. Levitated optomechanical systems are suitable for achieving ultra-low decoherence by eliminating mechanical support, and resolving the free-fall problem mentioned in the introduction. The conventional method to prepare such a system is to levitate nanoparticles with optical tweezers [40]. However, there is a limitation that the mass of the particle can be only up to nanogram scales due to the size of the trapping beam [41]. To levitate larger masses suitable for gravity experiments, optical levitation of cavity mirrors is promising [31, 42]. It has been shown that these methods can levitate mirrors at milligram scale masses, and milligram scale is considered to be sweet spot for probing quantum nature of gravity [26–28]. In such cavity optomechanical systems, inverted oscillators can be prepared by an optical anti-spring based on cavity detuning [29, 30] or on cavity geometry [43, 44]. We first show that optical anti-spring based on cavity detuning leads to large decoherence due to photon shot noise. We then show that geometric anti-spring can significantly suppress decoherence, and study

levitated mirrors in a sandwich configuration [31] as an example of experimental realization.

A. Anti-spring effect of detuned cavity

In cavity optomechanics, optical anti-spring can be generated by injecting a red-detuned laser beam. The resonant frequency in the longitudinal direction of the anti-spring mirror due to detuning $\Delta \equiv \omega_\ell - \omega_{\text{cav}} < 0$ is [29]

$$\omega_{\text{opt}}^2 = \frac{4\omega_\ell P_{\text{cav}}}{mcL\kappa} \frac{\Delta/\kappa}{[1 + (\Delta/\kappa)^2]^2}, \quad (17)$$

where ω_ℓ is the laser frequency, ω_{cav} is the cavity resonant frequency, P_{cav} is the intracavity power, L is the cavity length, and κ is the amplitude decay rate of the cavity. Here, we assumed that the intrinsic mechanical frequency is negligibly smaller than $|\omega_{\text{opt}}|$.

However, the quantum fluctuation of the radiation pressure of the intracavity photons, namely photon shot noise, leads to a new source of decoherence. Its corresponding decoherence parameter is (see Appendix B for derivation)

$$\mu_{\text{shot}} = \frac{\kappa}{|\Delta|}. \quad (18)$$

Making μ_{shot} smaller than η in Eq. (1) would be experimentally challenging, as it would require extremely large detuning of $|\Delta|/\kappa \sim 10^{13}$. Moreover, from Eq. (17) such large detuning makes ω_{opt} tiny, which leads to longer τ_{ent} . Therefore, optical anti-spring based on cavity detuning is not suitable for our purpose.

B. Levitated mirrors in sandwich configuration

To address the shot noise problem seen above, we now consider the anti-spring effect based on the cavity geometry in the transversal motion of the mirror. The shot noise can be significantly reduced, as the intracavity photons push the mirrors in a longitudinal direction.

Optical levitation of mirrors in a sandwich configuration illustrated in Fig. 3 is an example of experimental realizations that can create anti-spring in the transversal motion of levitated mirrors [31, 45]. The upper and lower mirrors are fixed and compose two Fabry-Pérot cavities with the levitated mirror at the center. To keep its levitation, we need to satisfy

$$mg = \frac{2}{c} (P_L - P_U), \quad (19)$$

where g is the gravitational acceleration and $P_{L/U}$ is the intracavity power of the lower/upper cavity. Since the levitated mirror is convex downward, the lower and upper

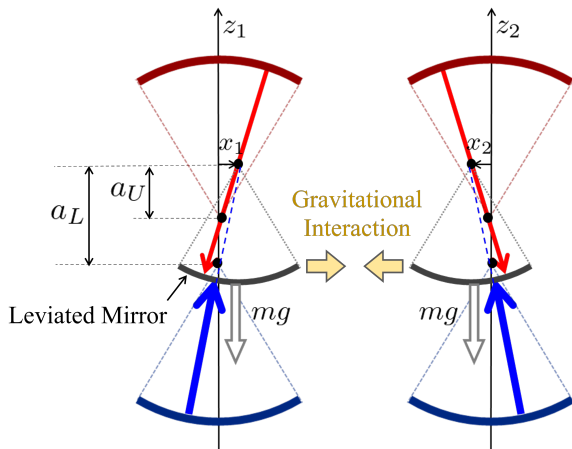


FIG. 3: Our working example of an optomechanical setup. Three vertically aligned mirrors form a sandwich configuration. The upper and lower mirrors are fixed. They constitute two cavities (red and blue) that levitate the center mirror and control the stability of its horizontal motion. After preparing the initial static state of the levitated mirror in a trapping potential, one can instantly switch the optics parameters and place the levitated mirror in an unstable potential for the horizontal direction. We arrange two of these configurations side by side and let the levitated mirrors gravitationally interact until they generate detectable entanglement.

cavity destabilizes and stabilizes its horizontal motion, respectively. The resonant frequency of the center mirror in the horizontal direction is

$$\begin{aligned} \omega_{\text{hor}}^2 &= \frac{2}{mc} \left(\frac{P_U}{a_U} - \frac{P_L}{a_L} \right) = \frac{2(a_L - a_U)}{mc a_U a_L} P_L - \frac{g}{a_U}, \quad (20) \\ &\simeq -(1\text{kHz})^2 \left(\frac{m}{0.1\text{mg}} \right)^{-1} \left(\frac{P_L}{30\text{kW}} \right) \left(\frac{a_L}{2\text{mm}} \right)^{-1}, \quad (21) \end{aligned}$$

where $a_{L/U}$ is the distance between the centers of curvature of the levitated mirror and the lower/upper mirror, and we used Eq. (19) for the second equation. When ω_{hor}^2 is negative (positive), the levitated mirror behaves as an inverted (harmonic) oscillator. To prepare the initial state in a harmonic potential and then to switch to an inverted oscillator, we can effectively change a_U , as described in Appendix C. The frequency of the inverted oscillator is evaluated in the second line of Eq. (21), where we ignored the contribution from P_U , because the P_L term dominates after the change of a_U .

Now we evaluate the decoherence effect of the shot noise in the horizontal direction. The lateral spread of the wave function of the levitated mirror at the time of the observable entanglement generation τ_{ent} is

$$\Delta x \simeq \frac{e^{\omega \tau_{\text{ent}}}}{\sqrt{2m\omega_{\text{in}}/\hbar}} \simeq 0.3\text{pm} \omega_{\text{kHz}}^{3/2} \left(\frac{m}{0.1\text{mg}} \right)^{-\frac{1}{2}} \left(\frac{\omega_{\text{in}}}{1\text{MHz}} \right)^{-1}, \quad (22)$$

where $\omega = |\omega_{\text{hor}}|$ is the frequency of the inverted potential, and ω_{in} is the frequency of the initial trapping potential in which the oscillators reached the ground state. When this initial potential is deep $\chi \equiv \omega_{\text{in}}/\omega \gg 1$, the initial uncertainty (7) reads $\sigma(0) \equiv \text{diag}[\chi^{-1}, \chi, \chi^{-1}, \chi]/2$ and then $e^{\omega \tau_{\text{ent}}}$ shrinks by $\sqrt{2/\chi}$ compared to Eq. (13) (see Eq. (30) in Appendix A). Eq. (22) accounts for this effect.

The shot noise from the lower cavity, which is louder than the upper cavity, is suppressed at least by a factor of $(\Delta x/a_L)^2$. We obtain the decoherence parameter as

$$\begin{aligned} \mu_{\text{shot,hor}} &= \frac{16\omega_\ell P_L}{m\omega^2 c^2 T_{\text{in}}} \left(\frac{\Delta x}{a_L} \right)^2 \simeq \frac{8\omega_\ell \Delta x^2}{ca_L T_{\text{in}}}, \\ &= 2.5 \times 10^{-14} \omega_{\text{kHz}}^3 \left(\frac{a_L}{2\text{mm}} \right)^{-1} \left(\frac{m}{0.1\text{mg}} \right)^{-1} \left(\frac{\omega_{\text{in}}}{1\text{MHz}} \right)^{-2}, \quad (23) \end{aligned}$$

where we use Eq. (21) for the second equation, the laser wavelength of 1064nm, and the power transmittance of the cavity input mirrors $T_{\text{in}} = 0.1$. Compared to the single detuned cavity case (18), the decoherence effect of the shot noise is dramatically reduced. Unfortunately, the ω dependence of $\mu_{\text{shot,hor}}$ has a positive power, and a larger ω leads to quicker decoherence. To fully take advantage of the short time scale τ_{ent} studied in Sec. III, one needs to devise another way to suppress the shot noise decoherence. Nevertheless, our setup serves as proof of principle that an inverted oscillator with ultra-low decoherence can be realized in optomechanical systems.

To measure the gravity-induced entanglement, we place two copies of the sandwich configuration next to each other. We initially trap the levitated mirrors in a harmonic potential and then let the levitated mirrors gravitationally interact in the inverted potential by instantly switching the parameter a_U . After τ_{ent} has passed, we measure their horizontal momenta and positions. This operation should be repeated for many times to significantly detect the logarithmic negativity. Our setup allows for continuous iteration of the process by returning the potential to harmonic form after the measurement, as the mirrors do not free-fall. The short τ_{ent} of the inverted oscillators is also beneficial in speeding up this cycle.

V. CONCLUSION

In this paper, we studied two oscillators with arbitrary quadratic potentials and calculated the gravity-induced entanglement between them. No particular gain was found by considering asymmetric oscillators. We found that the logarithmic negativity for the identical oscillators reduces to a simple form, $E_N \simeq 3(\eta - \mu)f_{\text{gra}}$, in the long-time regime. As shown in Fig. 2, f_{gra} strongly

depends on the potential form characterized by λ . Remarkably, inverted oscillators ($\lambda = -1$) have exponentially growing f_{gra} , which generate entanglement most quickly and are most resistant to decoherence. The short time scale τ_{ent} of the inverted oscillators would also help to avoid decoherence from molecular collisions.

We also investigated experimental realizations of inverted oscillators in levitated optomechanics. We pointed out that the anti-spring by detuning in a single cavity suffers from quick decoherence due to photon shot noise. Then, we considered a sandwich configuration, which geometrically creates the anti-spring. It enables us to dramatically suppress shot noise decoherence because gravity acts in the horizontal direction while the laser direction is vertical. We also noted that our optomechanical setup allows repetitive measurement cycles and solves the free-fall problem. Our idea of using instability to dramatically shorten the time scale opens up new possibilities for experimental tests of the quantum nature of gravity.

ACKNOWLEDGEMENT

We would like to thank Miles P. Blencowe for fruitful discussions. This work was supported in part by the Japan Society for the Promotion of Science (JSPS) KAKENHI, Grants No. JP23K03424 (T.F.), JP23K13103 (A.M.), JP20H05854 (T.F.&Y.M.), by JST PRESTO Grant No. JPMJPR200B (Y.M.), and by the Nagoya University Interdisciplinary Frontier Fellowship (Y.K.).

Appendix A. Solution for the coupled oscillators

With the variable $u(t)$ in Eq. (6), the Heisenberg-Langevin equations (4) can be rewritten as

$$\dot{u}(t) = K u(t) + \ell(t), \quad (24)$$

with

$$K \equiv \begin{pmatrix} 0 & \omega & 0 & 0 \\ \omega(\eta - \lambda_1) & 0 & -\omega\eta & 0 \\ 0 & 0 & 0 & \omega \\ -\omega\eta & 0 & \omega(\eta - \lambda_2) & 0 \end{pmatrix}, \quad \ell(t) = \begin{pmatrix} 0 \\ \xi_1 \\ 0 \\ \xi_2 \end{pmatrix}, \quad (25)$$

where we employed matrix representation. Its analytic solution is found as

$$u(t) = W_+(t)u(0) + W_+(t) \int_0^t dt' W_-(t') \ell(t'), \quad (26)$$

with $W_{\pm}(t) \equiv e^{\pm Kt}$. The covariance matrix (7) is also obtained as

$$\sigma(t) = W_+(t)\sigma(0)W_+^T(t) + W_+(t) \left[\int_0^t dt' W_-(t') D W_-^T(t') \right] W_+^T(t), \quad (27)$$

with $D \equiv \text{diag}(0, \mu\omega, 0, \mu\omega)$. We numerically evaluate the logarithmic negativity (10) of this solution and draw Fig. 1.

After setting $\lambda \equiv \lambda_1 = \lambda_2$, by calculating the minimum symplectic eigenvalue and expanding it with respect to small parameters $\eta \sim \mu \ll 1$, we find

$$\tilde{\nu}_{\text{min}} - \frac{1}{2} = -\eta f_{\text{gra}}(t) + \mu f_{\text{dec}}(t) + \mathcal{O}(\eta^2, \mu^2). \quad (28)$$

The full expressions for f_{gra} and f_{dec} are given by

$$f_{\text{gra}} = \frac{1}{8\sqrt{2}\lambda^{3/2}} \left[\mathcal{C}_1 + \mathcal{C}_2 \cos(2\sqrt{\lambda}t\omega) + \mathcal{C}_3 \sin(2\sqrt{\lambda}t\omega) + \mathcal{C}_4 \cos(4\sqrt{\lambda}t\omega) \right]^{1/2}, \\ f_{\text{dec}} = \frac{2\sqrt{\lambda}(\lambda + 1)\omega t + (\lambda - 1) \sin(2\sqrt{\lambda}\omega t)}{8\lambda^{3/2}}, \quad (29)$$

with $\mathcal{C}_1 = 1 + \lambda(\lambda + 8(\lambda - 1)^2\omega^2 t^2 + 14)$, $\mathcal{C}_2 = -16\lambda$, $\mathcal{C}_3 = 8\sqrt{\lambda}(\lambda^2 - 1)\omega t$, and $\mathcal{C}_4 = -(\lambda - 1)^2$. Plugging $\lambda = 0, \pm 1$ and further taking the long time limit, $\omega t \gg 1$, one finds Eq. (12).

With a different initial covariance matrix $\sigma(0) = \text{diag}[\chi^{-1}, \chi, \chi^{-1}, \chi]/2$, one can repeat the same procedure and finds

$$f_{\text{gra}} = \frac{1}{8\sqrt{2}\chi} \left[8t^2(\chi^2 + 1)^2\omega^2 - \chi^4 + 14\chi^2 - 1 - 16\chi^2 \cosh(2t\omega) - 8(\chi^4 - 1)\omega t \sinh(2\omega t) + (\chi^2 + 1)^2 \cosh(4\omega t) \right]^{1/2}, \\ f_{\text{dec}} = \frac{(\chi^2 + 1) \sinh(2\omega t) - 2(\chi^2 - 1)\omega t}{8\chi}, \quad (30)$$

for $\lambda = -1$. In the long time limit $\omega t \gg 1$, they read $f_{\text{gra}} \simeq f_{\text{dec}} \simeq (\chi^2 + 1)e^{2\omega t}/16\chi$ and are approximated by $\chi e^{2\omega t}/16$ for $\chi \gg 1$. Compared to Eq. (12), f_{gra} becomes larger by a factor of $\chi/2$ and thus $e^{\omega\tau_{\text{ent}}}$ is smaller by $\sqrt{2/\chi}$. Note that the same result can be obtained by making the replacements $\omega \rightarrow \omega/\sqrt{|\lambda|}$, $\eta \rightarrow |\lambda|\eta$ and taking the limit of $|\lambda| \ll 1$ in Eqs. (11) and (29) with $|\lambda| = \chi^2$.

Appendix B. Decoherence from shot noise in detuned cavities

The intracavity power fluctuates due to the intrinsic shot noise of the laser beam as

$$\delta P_{\text{cav}} = \sqrt{2\hbar\omega\ell} \frac{P_{\text{cav}}}{P_{\text{in}}}, \quad (31)$$

where $P_{\text{cav}} = 4P_{\text{in}}/(T_{\text{in}}[1 + (\Delta/\kappa)^2])$ is the intracavity power. The corresponding one-sided power spectrum density of the force is

$$S_{\text{shot}}^F = \left(\frac{2\delta P_{\text{cav}}}{c} \right)^2 = \frac{32\hbar\omega\ell P_{\text{cav}}}{c^2 T_{\text{in}} [1 + (\Delta/\kappa)^2]}. \quad (32)$$

The decoherence parameter μ can be computed as

$$\mu_{\text{shot}} = \frac{S_{\text{shot}}^F}{2\hbar m \omega^2} = \frac{16\omega_L P_{\text{cav}}}{\omega^2 m c^2 T_{\text{in}} [1 + (\Delta/\kappa)^2]}. \quad (33)$$

Substituting $|\omega_{\text{opt}}|$ of Eq. (17) into ω in the above equation and using $T_{\text{in}} = 4L\kappa/c$, which ignores the intracavity loss, we obtain Eq. (18). Since both ω_{opt}^2 and S_{shot}^F scales linearly with optomechanical coupling strength, Eq. (18) will be only dependent on normalized detuning.

Appendix C. Setup for switching potentials

The expression for the frequency of the levitated mirror in the horizontal direction ω_{hor}^2 in Eq. (20) implies that changing the intracavity power P_L alone cannot convert a harmonic potential to a high-frequency inverted potential, because the coefficient of P_L remains negative for $a_L < a_U$. To prepare the initial state and start the evolution of the coupled oscillators, it is crucial that our system can provide both harmonic and inverted potentials, as well as quickly switch between them.

This can be done, for example, by an experimental setup illustrated in Fig. 4. There are two upper cavities formed by an upper mirror labeled UM1(UM2) and the levitation mirror. The first upper cavity has a distance between the centers of curvature of a_{U1} which meets $a_L > a_{U1}$, to create a harmonic potential, and the second upper cavity has a_{U2} which meets $a_L < a_{U2}$, to create an inverted potential. Two cavities have different polarizations to avoid coupling between two cavities, and a polarizing beamsplitter is inserted in the cavity to share the same levitation mirror. By switching relative intracavity power between the first and the second upper cavities by an acousto-optic modulator (AOM), we can effectively switch between harmonic and inverted potentials. The typical speed for the switch is less than 100 nsec for an AOM, which is much faster than the time required to generate the entanglement in Eq. (13).

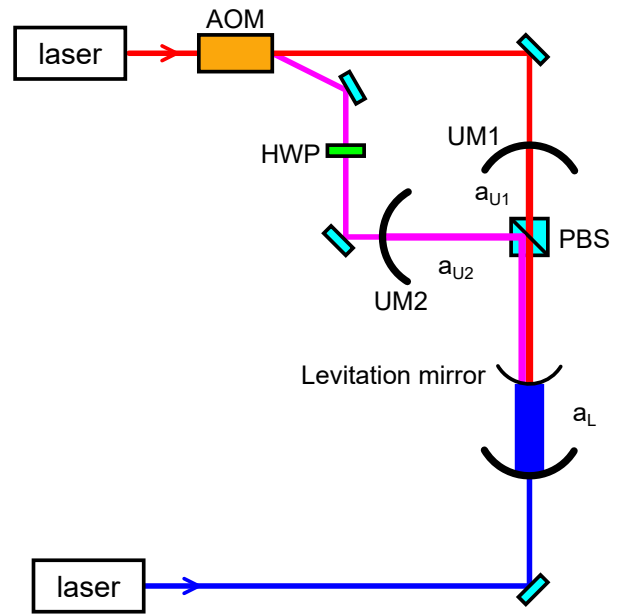


FIG. 4: Example setup for effectively changing a_U . AOM: acousto-optic modulator, HWP: half-wave plate, PBS: polarizing beamsplitter.

Evidence of Quantum Effects in Gravity”, *Phys. Rev. Lett.* **119**, (2017) 240402.

* Electronic address: tomofuji@aoni.waseda.jp

† Electronic address: kaku.yuka.g4@s.mail.nagoya-u.ac.jp

‡ Electronic address: matsumura.akira@phys.kyushu-u.ac.jp

§ Electronic address: yuta@caltech.edu

- [1] C. Kiefer, “Quantum gravity: general introduction and recent developments”, *Ann. Phys.* **15**, 129 (2006)
- [2] R. P. Woodard, “How far are we from the quantum theory of gravity?”, *Rep. Prog. Phys.* **72**, 126002 (2009)
- [3] S. Bose, A. Mazumdar, G. W. Morley, H. Ulbricht, M. Toroš, M. Paternostro, A. A. Geraci, P. F. Barker, M. S. Kim, and G. Milburn, “Spin Entanglement Witness for Quantum Gravity”, *Phys. Rev. Lett.* **119**, (2017) 240401.
- [4] C. Marletto and V. Vedral, “Gravitationally Induced Entanglement between Two Massive Particles is Sufficient

- [5] T. W. van de Kamp, R. J. Marshman, S. Bose, and A. Mazumdar, “Quantum gravity witness via entanglement of masses: Casimir screening”, *Phys. Rev. A* **102**, 062807 (2020).
- [6] M. Toroš, T. W. van de Kamp, R. J. Marshman, M. S. Kim, A. Mazumdar, and S. Bose, “Relative acceleration noise mitigation for nanocrystal matter-wave interferometry: Applications to entangling masses via quantum gravity”, *Phys. Rev. Research* **3**, 023178 (2021).
- [7] H. Chevalier, A. J. Paige, and M. S. Kim, “Witnessing the nonclassical nature of gravity in the presence of unknown interactions”, *Phys. Rev. A* **102**, 022428 (2020).
- [8] H. C. Nguyen and F. Bernards, “Entanglement dynamics of two mesoscopic objects with gravitational interaction”, *Eur. Phys. J. D* **74**, 69 (2020).
- [9] D. Miki, A. Matsumura and K. Yamamoto, “Entanglement and decoherence of massive particles due to gravity”, *Phys. Rev. D* **103**, 026017 (2021).
- [10] J. Tilly, R. J. Marshman, A. Mazumdar, and S. Bose, “Qudits for witnessing quantum-gravity-induced entanglement of masses under decoherence”, *Phys. Rev. A* **104**, 052416 (2021).
- [11] T. Krisnanda, G. Y. Tham, M. Paternostro, and T. Paterek, “Observable quantum entanglement due to gravity”, *npj Quant. Inf.* **6**, 12 (2020).
- [12] S. Qvarfort, S. Bose, and A. Serafini, “Mesoscopic entanglement through central-potential interactions”, *J. Phys. B* **53**, 235501 (2020).
- [13] A. A. Balushi, W. Cong, and R. B. Mann, “Optomechanical quantum Cavendish experiment”, *Phys. Rev. A* **98**, (2018) 043811.
- [14] H. Miao, D. Martynov, H. Yang, and A. Datta, “Quantum correlations of light mediated by gravity”, *Phys.*

- Rev. A* **101**, (2020) 063804.
- [15] C. Wan, “Quantum superposition on nano-mechanical oscillator”, PhD thesis (Imperial College London, 2017)
- [16] A. Matsumura and K. Yamamoto, “Gravity-induced entanglement in optomechanical systems”, *Phys. Rev. D* **102**, 106021 (2020).
- [17] A. Datta and H. Miao, “Signatures of the quantum nature of gravity in the differential motion of two masses” *Quantum Sci. Technol.* **6**, 045014 (2021)
- [18] D. Miki, A. Matsumura and K. Yamamoto, “Non-Gaussian entanglement in gravitating masses: the role of cumulants”, *Phys. Rev. D* **105**, 026011 (2022).
- [19] Y. Kaku, T. Fujita and A. Matsumura, “Enhancement of quantum gravity signal in an optomechanical experiment”, arXiv:2306.02974.
- [20] A. Matsumura, Y. Nambu and K. Yamamoto, “Leggett-Garg inequalities for testing quantumness of gravity”, *Phys. Rev. A* **106**, 012214 (2022).
- [21] D. Carney, H. Müller, and J. M. Taylor, “Using an Atom Interferometer to Infer Gravitational Entanglement Generation”, *PRX Quantum* **2**, 030330 (2021).
- [22] D. Carney, H. Müller, and J. M. Taylor, “Erratum: Using an atom interferometer to infer gravitational entanglement generation [PRX Quantum 2, 030330 (2021)]”, *PRX Quantum* **3**, 010902(2022).
- [23] K. Streltsov, J. S. Pedernales, and M. B. Plenio, “On the Significance of Interferometric Revivals for the Fundamental Description of Gravity”, *Universe* **8**, 58 (2022).
- [24] J. S. Pedernales, K. Streltsov, and M. B. Plenio, “Enhancing Gravitational Interaction between Quantum Systems by a Massive Mediator”, *Phys. Rev. Lett.* **128**, 110401 (2022).
- [25] S. Rijavec, M. Carlesso, A. Bassi, V. Vedral, and C. Marletto. “Decoherence effects in non-classicality tests of gravity”, *New J. Phys.* **23**, 4, 043040 (2021).
- [26] J. Schmöle, M. Dragosits, H. Hepach, and M. Aspelmeyer, “A micromechanical proof-of-principle experiment for measuring the gravitational force of milligram masses” *Class. Quantum Grav.* **33**, 125031 (2016)
- [27] N. Matsumoto, S. B. Cataño-Lopez, M. Sugawara, S. Suzuki, N. Abe, K. Komori, Y. Michimura, Y. Aso, and K. Edamatsu, “Demonstration of Displacement Sensing of a mg-Scale Pendulum for mm- and mg-Scale Gravity Measurements” *Phys. Rev. Lett.* **122**, 071101 (2019)
- [28] T. Westphal, H. Hepach, J. Pfaff and M. Aspelmeyer, “Measurement of gravitational coupling between millimetre-sized masses” *Nature* **591**, 225–228 (2021)
- [29] Y. Chen, “Macroscopic Quantum Mechanics: Theory and Experimental Concepts of Optomechanics”, *J. Phys. B* **46**, 104001 (2013).
- [30] M. Aspelmeyer, T. J. Kippenberg, and F. Marquardt, “Cavity optomechanics”, *Rev. Mod. Phys.* **86**, (2014) 1391.
- [31] Y. Michimura, Y. Kuwahara, T. Ushiba, N. Matsumoto, and M. Ando “Optical levitation of a mirror for reaching the standard quantum limit” *Optics Express* **25**, 12, 13799-13806 (2017)
- [32] G. Vidal and R. Werner, “Computable measure of entanglement”, *Phys. Rev. A* **65**, (2002) 032314.
- [33] M. Horodecki, R. Horodecki, and P. Horodecki, “Separability of mixed states: necessary and sufficient conditions”, *Phys. Lett. A* **223**, (1996) 1-8.
- [34] A. Peres, “Separability Criterion for Density Matrices”, *Phys. Rev. Lett.* **77**, (1996) 1413.
- [35] R. Simon, “Peres-Horodecki Separability Criterion for Continuous Variable Systems”, *Phys. Rev. Lett.* **84**, 2726 (2000).
- [36] G. Giedke, L. M. Duan, J. I. Cirac, and P. Zoller, “Distillability criterion for all bipartite Gaussian states”, *Quantum Inf. Comput.* **1**, 79 (2001).
- [37] T. A. Palomaki, J. D. Teufel, R. W. Simmonds, AND K. W. Lehnert, “Entangling Mechanical Motion with Microwave Fields” *Science* **342**, 6159, 710-713 (2013)
- [38] M. Schlosshauer, “Decoherence and the Quantum-To-Classical Transition” *Springer*, Berlin (2007)
- [39] S. Sellner, M. Besirli, M. Bohman, M. J. Borchert, J. Harrington, T. Higuchi, A. Mooser, H. Nagahama, G. Schneider, C. Smorra, T. Tanaka, K. Blaum, Y. Matsuda, C. Ospelkaus, W. Quint, J. Walz, Y. Yamazaki and S. Ulmer, “Improved limit on the directly measured antiproton lifetime” *New J. Phys.* **19**, 083023 (2017)
- [40] G. Winstone, M. Bhattacharya, A. A. Geraci, T. Li and P. J. Pauzauskie, “Levitated optomechanics: A tutorial and perspective” arXiv: 2307.11858
- [41] D. G. Grier, “A revolution in optical manipulation” *Nature* **424**, 810–816 (2003)
- [42] G. Guccione, M. Hosseini, S. Adlong, M. T. Johansson, J. Hope, B. C. Buchler, and P. K. Lam, “Scattering-Free Optical Levitation of a Cavity Mirror” *Phys. Rev. Lett.* **111**, 183001 (2013)
- [43] S. Solimeno, F. Barone, C. de Lisio, L. Di Fiore, L. Milano, and G. Russo, “Fabry-Pérot resonators with oscillating mirrors” *Phys. Rev. A* **43**, 6227 (1991)
- [44] J. A. Sidles and D. Sigg, “Optical torques in suspended Fabry–Perot interferometers” *Phys. Let. A* **354**, 3, 167-172 (2006)
- [45] T. Kawasaki, N. Kita, K. Nagano, S. Wada, Y. Kuwahara, M. Ando, and Y. Michimura, “Optical trapping of the transversal motion for an optically levitated mirror” *Phys. Rev. A* **102**, 053520 (2020)